MICROSTRUCTURE ANALYSIS OF SILK SAMPLES USING MUELLER MATRIX DETERMINATION AND SPARSE REPRESENTATION

Xiaomin Zhang[1,2], *Fei Zhou*[1,2,⋆], *Yang Dong*[1], *Hui Ma*[1], *Qingmin Liao*[1,2]

[1]Graduate School at Shenzhen, Tsinghua University, Shenzhen, China
[2]Department of Electronic Engineering, Tsinghua University, China

ABSTRACT

In this paper, we propose to use Mueller matrix determination and sparse representation to classify silk samples washed in different detergents. Different detergents have different effects on the same silk samples after washing, and we distinguish their diversities in the Mueller matrix images(MMI) instead of visible light images(VLI). Compared with VLI, Mueller matrix, also known as polarization image, reflects the wavelength-scale microstructure and some optical properties of samples, and focuses on extracting the index to research the polarization property. To achieve a good performance with the microstructure analysis, we utilize the method of sparse representation which uses the reconstruction error for classification. Generally speaking, we introduce to combine Mueller matrix with sparse representation in the classification of the same silk samples washed in different detergents, and the high precision in experimental results indicates that our method works well.

Index Terms— Mueller matrix, sparse representation, silk, classification

1. INTRODUCTION

Although the development of imaging technology improves constantly, the existing visible light imaging technology cannot present microstructural information. It is worth mentioning that polarization imaging contains abundant microstructural information, because the polarization changing of light for scatter is sensitive to the microstructural features of wavelength scale in the process of polarized light scattering. Polarized imaging has widespread applications, such as atmospheric remote sensing[1],[2], astronomy[1],[3], biomedical diagnostics[4],[5],[6], and so on.

Mueller matrix polarimetry can powerfully reflect the wavelength-scale microstructure and some optical properties of samples[7],[8]. There are 16 elements in Mueller matrix, yet we generally pay close attention to the element of m_{11} containing visible light information and ignore other elements as the human eyes are insensitive to light. However, more optical properties hide in the other 15 elements. Mueller matrix polarimetry may also serve as a powerful tool to distinguish the characteristic features of different textile samples, such as acetate, cotton, silk, and ramie[9]. In recent studies, Mueller matrix parameters have been used to provide comprehensive characterization of the polarization features to assist various pathological detections, such as skin cancer [10], cervical cancer[11], liver fibrosis[12], and so on[13],[14]. But the applications of taking Mueller matrix as images to achieve recognition and classification have not been reported in the literature.

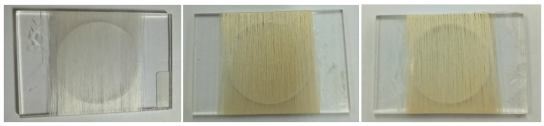

(a) (b) (c)

Fig. 1. VLI of silk sample and its counterparts washed by six times. (a)Original silk sample. (b)Washed by laundry powder. (c)Washed by toilet soap.

Sparse representation is an algorithm introduced by Olshausen[15]. The core idea of sparse representation is to find a high-level representation of the input signal[15]. It needs to learn a dictionary called basis functions, and the input signal can be represented by the linear combination of the basis functions while the coefficient vectors are sparse. Recently , sparse coding are used in various fields, especially in image processing such as image noise reduction, image classification, texture classification and face recognition[16],[17].

In this paper, our contribution is to discuss the effects of different detergents on the microstructure of silk samples through the methods of sparse coding and Mueller matrix polarimetry. The diversities of silk samples can be revealed by Mueller matrix polarimetry and can be distinguished by using a sparse coding based classifier. The silk samples are washed several times by different detergents respectively, including fabric softener, laundry powder, toilet soap, fabric clean agent

This work was supported by the National Natural Science Foundation of China under Grant No.61527826, and the Special Foundation for the Development of Strategic Emerging Industries of Shenzhen under J-CYJ20150331151358138.

⋆ Corresponding author: flying.zhou@163.com

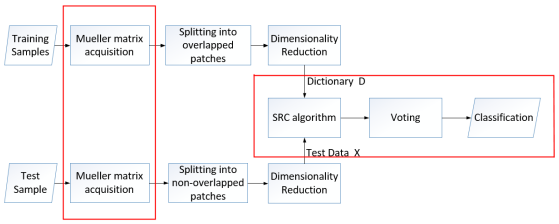

Fig. 2. Overall system framework of the proposed method .

and soap powder. The 2D backscattering MMI and grayscale images are taken after each washing process. The samples washed in different detergents cannot be well distinguished through the grayscale images but satisfied classification can be achieved through MMI.

2. PROPOSED METHOD

2.1. Conventional visible light images

Silk samples are prepared by wrapping the silk fibers around a glass slide as shown in Fig.1. We can observe that silk samples washed by detergents become light yellow because yellowing is a typical characterization of protein denaturation. However, we find no obvious differences between the VLI of silk samples which washed by laundry powder or toilet soap in Fig.1. Similarly, we cannot visually distinguish what kind of detergent washing the silk samples in the grayscale images.

2.2. Overall system and motivation

In order to distinguish silk samples washed by different detergents, we propose a new framework with MMI and a sparse coding based classifier, shown in Fig.2. We will emphatically introduce the details in the red frame.

Through the block of "Mueller matrix acquisition", MMI can be transformed from grayscale images. This part will be discussed in Section 2.3. We can get available dictionary **D** and test data **x** after reducing dimensions and extracting features in MMI. Then we set up a sparse coding based classifier and project a voting rule to implement classification. This part will be demonstrated in Section 2.4.

2.3. Mueller matrix acquisition

In the block of Mueller matrix acquisition, we use the dual rotating retarder configuration for 2D backscattering Mueller matrix measurements in [18]. As shown in Fig.3, the linear polarizer (P1, extinction ratio $>$ 1000:1, Daheng Optic, Beijing, China) and the quarter-wave plate (R1, Daheng Optic) control the polarization state of the incident light from the LED (633 nm, 3 W). Then the sample is illuminated by the collimated light of different polarization states and

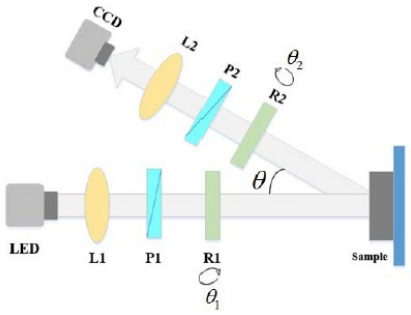

Fig. 3. Schematic of experimental setup for the backscattering Mueller matrix measurement.P1,P2: polarizer; R1,R2: quarter-wave plate; L1,L2: lens. The diameter of the illumination area is about 1.8 cm.

the backscattered photons pass through another quarter-wave plate (R2, Daheng Optic) and linear polarizer (P2, extinction ratio $>$ 1000:1, Daheng Optic). Finally the photons are collected by a CCD camera (QImaging 32-0122A, 12 bit, Surrey, BC, Canada). In order to avoid the surface reflection from the sample, it installs an oblique angle $\theta = 15^\circ$ between the illuminating and detection.

During the measurements, the polarizers (P1, P2) are fixed in the horizontal direction, and the two retarders (R1, R2) rotate with a fixed rate. After rotations of both retarders in fixed times, the Mueller matrix elements can be calculated. T is the total rotation of the first retarder in the measurement cycle(typically π or 2π), and Q is the total number of measurements within one measurement cycle. In this paper, $T = \pi$ and $Q = 30$, and the hth ($0 \leq h \leq 29$) is obtained with the first retarder oriented at $h\theta_1$ and the second retarder at $5h\theta_1$.

The output irradiance is given by the first element of the output Stokes vector,$s_{0.out}(h)$.The expression for the measured irradiance I_h is expanded and rewritten to produce terms that correspond to the Fourier series expansion

$$s_{0.out}(h) = I_h = \frac{a_0}{2} + \sum_{n=1}^{12}(a_n \cos 2n\theta_2 h + b_n \sin 2n\theta_2 h). \tag{1}$$

The Fourier coefficients a_n and b_n are functions of the sixteen elements of the sample Mueller matrix. These expressions are inverted to give the Mueller matrix elements(m_{11}, m_{12}, m_{13}, m_{14}, m_{21}, m_{22}, m_{23}, m_{24}, m_{31}, m_{32}, m_{33}, m_{34}, m_{41}, m_{42}, m_{43}, m_{44}) in terms of the Fourier series coefficients[19]. Finally, the Mueller matrix of this sample is given by

$$\mathbf{M} = \begin{bmatrix} m_{11} & m_{12} & m_{13} & m_{14} \\ m_{21} & m_{22} & m_{23} & m_{24} \\ m_{31} & m_{32} & m_{33} & m_{34} \\ m_{41} & m_{42} & m_{43} & m_{44} \end{bmatrix}. \tag{2}$$

The imaging setup is calibrated by measuring the Mueller matrices of standard samples such as air before applying to

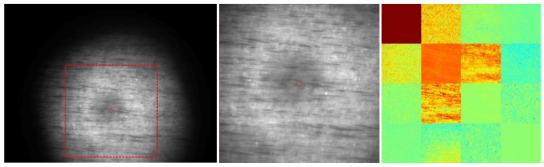

Fig. 4. Captured grayscale images and corresponding MMI of silk sample washed by laundry powder.(a) Actual picture. (b) Grayscale image in this study. (c) MMI.

the samples. The maximum errors for the absolute values of all the Mueller matrix elements are smaller than 0.01 after calibration.To better introduce the 2D backscattering MMI, we use a sample for example. This sample is washed in the laundry powder solution for one hour, and then completely dried out. We take the 2D backscattering MMI and grayscale images. The relationship between the actual picture, the used grayscale image, and MMI are shown in Fig.4. In Fig.4(a), the red box frame corresponds to each element of the Mueller matrix. All the matrix elements are normalized by the m_{11} to cancel lighting influences.

2.4. Classification strategy

MMI are obtained by Section 2.3, and then we process these MMI. The size of each element is seted as $G \times G$. According to the certain step by sliding window method, every element is segmented into many patches, which are overlapped. The size of patch is $g \times g$, and the step is *r* pixels. Next, we downsample by 2 for every patch of elements to reduce the noise and dimensions. The new matrix of each patch is transformed into a column vector. We combine all the column vectors in the array element to obtain the characteristic matrix which can represent the information. Next, for the same washed time $t_j, j \in \{0,1,2,3,4,5,6\}$, Mueller matrixes of *k* kinds of detergents are combined as $\mathbf{D}^{t_j} = \left[\mathbf{D}_1^{t_j}, \mathbf{D}_2^{t_j}, \cdots, \mathbf{D}_k^{t_j}\right]$ which is the dictionary in the time.

The test sample is washed by the same detergent as the one used in the training stage. The size of each element in MMI is $G \times G$, and the every element is segmented into many overlapped patches. The size of patch is $g \times g$. Through the dimensionality reduction, the result is the test sample's feature matrix $\mathbf{X} = [\mathbf{x}^1, \mathbf{x}^2, \cdots, \mathbf{x}^q]$.As the processing of 15 element(except m_{11} because its data is 1) is the same, we take the m_{12} element as an example to explain this method.

We set up a sparse coding based classifier, and the Sparse Representation Classification(SRC) algorithm is briefly introduced.

a.Input: a matrix of training samples$\mathbf{D} = [\mathbf{D}_1 ... \mathbf{D}_i ... \mathbf{D}_k]$, $\mathbf{D}_i \in \mathbf{R}^{N \times M}$ for k classes, $\mathbf{D}_i$ is the training set related to i-th class. A test sample is $\mathbf{x} \in \mathbf{R}^{N \times 1}$.

b.Normalize the columns of D to have unit $\mathbf{l^2}$ − norm.

c.Solve the $\mathbf{l^1}$ − minimization problem:

$$\hat{\mathbf{s}} = \arg\min_{\mathbf{s}} \|\mathbf{s}\|_1 \quad s.t. \|\mathbf{x} - \mathbf{D} \cdot \mathbf{s}\|_2 < \varepsilon \tag{3}$$

where constant ε is to account for the dense small noise in x, or to balance the coding error of $\mathbf{x}$ and the sparsity of $\mathbf{s}$.

d.Compute the residuals:

$$e_i(\mathbf{x}) = \|\mathbf{x} - \mathbf{D}_i\hat{\mathbf{s}}\|_2, \quad for\ i = 1, 2, \cdots, k \tag{4}$$

where $\hat{\mathbf{s}}$ denotes the coding coefficient vector associated with class *i*.

e.Output the identify of x as

$$identify(\mathbf{x}) = \arg\min_i \{e_i\}. \tag{5}$$

In this work, the optimization problem is adopted as

$$\min_s \|\mathbf{x} - \mathbf{D} \cdot \mathbf{s}\|_2^2 + \lambda\|\mathbf{s}\|_1 \tag{6}$$

where $\mathbf{D} = [\mathbf{D}_1, \mathbf{D}_2, \cdots, \mathbf{D}_k]$ is the dictionary,*k* is the number of categories. $\mathbf{s}$ is sparse representation vector, and λ is a balanced coefficient.

With determining the number of washing time t_j, inputs are test sample's feature vector $\mathbf{x}^q$,$q \in \{1, 2, 3, ..., 361\}$ and the dictionary $\mathbf{D}^{t_j}$, then we can receive sparse matrix $\mathbf{S} = [\mathbf{s}_1, \mathbf{s}_2, ..., \mathbf{s}_k]$. Next, reconstruction error is computed to obtain the identify of $\mathbf{x}$ as

$$\begin{aligned} e(\mathbf{x}^q) &= |\mathbf{x}^q - \mathbf{D}_i \cdot \mathbf{s}_i|^2 \\ identify(\mathbf{x}^q) &= \arg\min_i \{e\} \end{aligned} \tag{7}$$

where *i* is the category, $\mathbf{x}^q$ is the q^{th} column of the test matrix, and $identify(\mathbf{x}^q) \in \{1, 2, ..., k\}$ is the class of the q^{th} column of the test matrix.

In the voting and classification, we get *q* classification results and $identify(\mathbf{x}^q) \in \{1, 2, ..., k\}$. With the number of the same $identify(\mathbf{x}^q)$ adding, the category corresponding to the maximum number is the class to which the element belongs. Similarly for other elements of Mueller Matrix we use the same manner to achieve this classification.

3. EXPERIMENT RESULTS

3.1. Training and test dataset

We prepared silk samples by wrapping the silk fibers[1] around the glass slide. Then the silk samples were washed six times using five common detergents: fabric softener[2], laundry powder[2], toilet soap[2], fabric clean agent[3]and soap powder[4].

[1]Provided by Guangxi Institute of Supervision and Testing on Product Quality, Nanning, Guangxi, China

[2]These detergents are the same with those used in [9]

[3]Liby Q/LBJT,Guangzhou Liby enterprise group,LTD,Guangzhou,China

[4]Diaopai WL-I QB/T2387-2008, Nice Group China, Lishui, China

Table 1. The results in grayscale images of silk sample washed after 1 time by fabric clean agent

Category	laundry powder	toilet soap	soap powder	fabric softener	fabric clean agent
Times	107	73	79	76	26

The silk samples were washed in the detergent solution for one hour, and then completely dried out naturally. During the washing processes, other factors kept the same, such as the water temperature, soaking time, drying time and so on. There were no significant changes in the appearance of the silk samples. After each washing, we took the 2D backscattering MMI and grayscale images of the silk samples and observed the differences of variations in two kinds of images.As to the parameters setting, we choose $G = 600$, $g = 60$, $r = 10$, and $k = 5$.

3.2. Evaluation Metrics

In this paper, we define a series of indexes to measure the results. The first index describes the number of minimum reconstruction errors of the correct class in the proportion of the total number of minimum reconstruction errors in the grayscale and MMI, denoted as α. As there are 16 elements in MMI, the second index is the element-classification correct rate meaning the number of correct element-classification in the proportion of the number of total element, donated as β. Since m_{11} is normalized, we use the remaining 15 elements to determine results. The third index γ measures final results. If the recognition is correct, then the value of γ is 1, otherwise $\gamma = 0$. Therefore, we can realize that the larger values of the indexes α,β,γ illustrate the results are better.

3.3. Effectiveness of the proposal

In order to verify effectiveness of the proposal, we use 17 test samples in this work. Here we take one test sample washed in one time by fabric clean agent for example. This reconstruction error can be calculated in our method and the number of occurrences of the minimum error is recorded. The sum of the number of occurrences of each category is given in the Table 1. Through the Table 1 we can know $\alpha \approx 7.20\%$ and $\gamma = 0$. The results can not accurately prove that the test sample to which category belongs. Then we use the Mueller matrix images to test this test sample.

We take this test sample's Mueller matrix image, calculate the reconstruction error, and record the number of occurrences of the minimum error. The sum of the number of occurrences of each category is given in the Table 2.

As can be seen from the Table 2 ,the element correct rate is $\beta = 14/15 \approx 93.33\%$, $\alpha \approx 78.10\%$, and $\gamma = 1$. It can be seen from the experimental results that, for all the array elements, the number of the minimum reconstructed errors is the most in the fifth category, it can be judged that the silk sample is washed by the fifth kind of cleaning agent.

Table 2. The results in MMI of silk sample Washed after 1 time by fabric clean agent

Elements	laundry powder	toilet soap	soap powder	fabric softener	fabric clean agent
m_{12}	94	2	67	1	197
m_{13}	0	0	0	0	361
m_{14}	211	0	0	0	150
m_{21}	59	0	54	1	247
m_{22}	18	26	12	2	303
m_{23}	44	49	65	28	175
m_{24}	4	0	2	0	355
m_{31}	0	0	0	0	361
m_{32}	62	25	89	15	170
m_{33}	24	16	58	2	261
m_{34}	16	1	25	0	319
m_{41}	0	0	1	0	360
m_{42}	3	1	7	0	350
m_{43}	17	3	18	2	321
m_{44}	10	0	51	1	299
Times	1	0	0	0	14

Table 3. Mean of α, β, γ on the 17 test samples

Mean of the indexes	α	β	γ
Grayscale images	28.32%	/	17.64%
Mueller matrix images	76.50%/	90.20%	100%

In this experiment, we use 17 test samples, each of which is washed by the five detergents respectively. The test sample satisfies robustness. Although some of elements are wrongly identified, they do not affect the finally correct conclusion. We also use their grayscale images to identify, but the result is not satisfactory. The results are shown in Table 3. It is also fully explained that we can use the MMI of the objects to obtain more micro-information to classify when using natural images can not be classified.

4. CONCLUSION

In this paper, our innovation is that we relate the Mueller matrix and a sparse coding based classifier to achieve the classification of silk washed by fabric softener, laundry powder, toilet soap, fabric clean agent and soap powder. In the previous literature, there is no report about using the Mueller matrices in classification task. The advantage of using polarized light and Mueller Matrix is that they could show more microstructure features, and through the diversity of Mueller Matrix images, we can classify this silk sample which can not be classified in the visible light images. In addition, this work achieves a satisfied correct recognition rate on 17 silk samples test. In the future, we will build a larger database and take more extensive experiments to demonstrate our method.

5. REFERENCES

[1] Frans Snik, Julia Craven-Jones, Michael Escuti, Silvano Fineschi, David Harrington, Antonello De Martino, Dimitri Mawet, Jérôme Riedi, and J Scott Tyo, "An overview of polarimetric sensing techniques and technology with applications to different research fields," in *SPIE Sensing Technology+ Applications*. International Society for Optics and Photonics, 2014, pp. 90990B–90990B.

[2] Brian Cairns, Edgar E Russell, Joseph D LaVeigne, and Philip MW Tennant, "Research scanning polarimeter and airborne usage for remote sensing of aerosols," in *Optical Science and Technology, SPIE's 48th Annual Meeting*. International Society for Optics and Photonics, 2003, pp. 33–44.

[3] Christoph U Keller, "Instrumentation for astrophysical spectropolarimetry," in *Astrophysical Spectropolarimetry*. Cambridge University Press, 2002, vol. 1, pp. 303–354.

[4] Tatiana Novikova, Angelo Pierangelo, Antonello De Martino, Abdelali Benali, and Pierre Validire, "Polarimetric imaging for cancer diagnosis and staging," *Optics and photonics news*, vol. 23, no. 10, pp. 26, 2012.

[5] Nirmalya Ghosh and I Alex Vitkin, "Tissue polarimetry: concepts, challenges, applications, and outlook," *Journal of biomedical optics*, vol. 16, no. 11, pp. 110801–11080129, 2011.

[6] Steven L Jacques, "Optical properties of biological tissues: a review," *Physics in medicine and biology*, vol. 58, no. 11, pp. R37, 2013.

[7] Sanaz Alali and Alex Vitkin, "Polarized light imaging in biomedicine: emerging mueller matrix methodologies for bulk tissue assessment," *Journal of biomedical optics*, vol. 20, no. 6, pp. 061104–061104, 2015.

[8] Honghui He, Minghao Sun, Nan Zeng, E Du, Shaoxiong Liu, Yihong Guo, Jian Wu, Yonghong He, and Hui Ma, "Mapping local orientation of aligned fibrous scatterers for cancerous tissues using backscattering mueller matrix imaging," *Journal of biomedical optics*, vol. 19, no. 10, pp. 106007–106007, 2014.

[9] Dong Yang, Honghui He, He Chao, Jialing Zhou, Zeng Nan, and Ma Hui, "Characterizing the effects of washing by different detergents on the wavelength-scale microstructures of silk samples using mueller matrix polarimetry:," *International Journal of Molecular Sciences*, vol. 17, no. 8, pp. 1301, 2016.

[10] E Du, Honghui He, Nan Zeng, Minghao Sun, Yihong Guo, Jian Wu, Shaoxiong Liu, and Hui Ma, "Mueller matrix polarimetry for differentiating characteristic features of cancerous tissues," *Journal of biomedical optics*, vol. 19, no. 7, pp. 076013–076013, 2014.

[11] Minghao Sun, Honghui He, Nan Zeng, E Du, Yihong Guo, Shaoxiong Liu, Jian Wu, Yonghong He, and Hui Ma, "Characterizing the microstructures of biological tissues using mueller matrix and transformed polarization parameters," *Biomedical optics express*, vol. 5, no. 12, pp. 4223–4234, 2014.

[12] Matthieu Dubreuil, Philippe Babilotte, Loïc Martin, David Sevrain, Sylvain Rivet, Yann Le Grand, Guy Le Brun, Bruno Turlin, and Bernard Le Jeune, "Mueller matrix polarimetry for improved liver fibrosis diagnosis," *Optics letters*, vol. 37, no. 6, pp. 1061–1063, 2012.

[13] Wenfeng Wang, Lee Guan Lim, Supriya Srivastava, Jimmy So Bok Yan, Asim Shabbir, and Quan Liu, "Roles of linear and circular polarization properties and effect of wavelength choice on differentiation between ex vivo normal and cancerous gastric samples," *Journal of biomedical optics*, vol. 19, no. 4, pp. 046020–046020, 2014.

[14] J Jagtap, S Chandel, N Das, J Soni, S Chatterjee, A Pradhan, and N Ghosh, "Quantitative mueller matrix fluorescence spectroscopy for precancer detection," *Optics letters*, vol. 39, no. 2, pp. 243–246, 2014.

[15] Bruno A Olshausen et al., "Emergence of simple-cell receptive field properties by learning a sparse code for natural images," *Nature*, vol. 381, no. 6583, pp. 607–609, 1996.

[16] Meng Yang, Lei Zhang, Jian Yang, and David Zhang, "Robust sparse coding for face recognition," in *Computer Vision and Pattern Recognition (CVPR), 2011 IEEE Conference on*. IEEE, 2011, pp. 625–632.

[17] Jostein Herredsvela, Kjersti Engan, Thor Ole Gulsrud, and Karl Skretting, "Texture classification using sparse representations by learned compound dictionaries," in *Workshop on Signal Processing with Adaptative Sparse Structured Representations. pp. TS1–4*, 2005.

[18] RMA Azzam, "Photopolarimetric measurement of the mueller matrix by fourier analysis of a single detected signal," *Optics Letters*, vol. 2, no. 6, pp. 148–150, 1978.

[19] David B Chenault, J Larry Pezzaniti, and Russell A Chipman, "Mueller matrix algorithms," in *San Diego'92*. International Society for Optics and Photonics, 1992, pp. 231–246.